European Journal of Pharmacology 782 (2016) 98–106

Contents lists available at ScienceDirect

European Journal of Pharmacology

journal homepage: www.elsevier.com/locate/ejphar

Molecular and cellular pharmacology

New thiazolidinediones affect endothelial cell activation and angiogenesis

Martina Rudnicki [a], Gustavo L. Tripodi [a], Renila Ferrer [a], Lisardo Boscá [b], Marina G.R. Pitta [c], Ivan R. Pitta [c], Dulcineia S.P. Abdalla [a,*]

[a] Department of Clinical and Toxicological Analyses, Faculty of Pharmaceutical Sciences, University of São Paulo, São Paulo, SP, Brazil
[b] Instituto de Investigaciones Biomédicas Alberto Sols (CSIC-UAM), Madrid, Spain
[c] Core of Therapeutic Innovation, Federal University of Pernambuco, Recife, PE, Brazil

ARTICLE INFO

Article history:
Received 25 January 2016
Received in revised form
8 April 2016
Accepted 20 April 2016
Available online 21 April 2016

Keywords:
Thiazolidinediones
Endothelial cells
Inflammation
Angiogenesis

ABSTRACT

Thiazolidinediones (TZDs) are peroxisome proliferator-activated receptor-γ (PPARγ) agonists used in treating type 2 diabetes that may exhibit beneficial pleiotropic effects on endothelial cells. In this study, we characterized the effects of three new TZDs [GQ-32 (3-biphenyl-4-ylmethyl-5-(4-nitro-benzylidene)-thiazolidine-2,4-dione), GQ-169 (5-(4-chloro-benzylidene)-3-(2,6-dichloro-benzyl)-thiazolidine-2,4-dione), and LYSO-7 (5-(5-bromo-1*H*-indol-3-ylmethylene)-3-(4-chlorobenzyl)-thiazolidine-2,4-dione)] on endothelial cells. The effects of the new TZDs were evaluated on the production of nitric oxide (NO) and reactive oxygen species (ROS), cell migration, tube formation and the gene expression of adhesion molecules and angiogenic mediators in human umbilical vein endothelial cells (HUVECs). PPARγ activation by new TZDs was addressed with a reporter gene assay. The three new TZDs activated PPARγ and suppressed the tumor necrosis factor α-induced expression of vascular cell adhesion molecule 1 and intercellular adhesion molecule 1. GQ-169 and LYSO-7 also inhibited the glucose-induced ROS production. Although NO production assessed with 4-amino-5-methylamino-2′,7′-difluorofluorescein-FM probe indicated that all tested TZDs enhanced intracellular levels of NO, only LYSO-7 treatment significantly increased the release of NO from HUVEC measured by chemiluminescence analysis of culture media. Additionally, GQ-32 and GQ-169 induced endothelial cell migration and tube formation by the up-regulation of angiogenic molecules expression, such as vascular endothelial growth factor A and interleukin 8. GQ-169 also increased the mRNA levels of basic fibroblast growth factor, and GQ-32 enhanced transforming growth factor-β expression. Together, the results of this study reveal that these new TZDs act as partial agonists of PPARγ and modulate endothelial cell activation and endothelial dysfunction besides to stimulate migration and tube formation.

1. Introduction

Vascular complications are a leading cause of diabetes-related morbidity and mortality (Rask-Madsen and King, 2013). Macrovascular complications, which mainly result from atherosclerosis, compromise arteries and augment the chance of critical limb ischemia, myocardial infarction, and stroke (Laakso and Kuusisto, 2014). In turn, microvascular complications have deleterious effects on eyes (Antonetti et al., 2012), kidneys (Zent and Pozzi, 2007), and nerves (Boulton et al., 2004) leading to blindness, end-stage renal disease, and lower leg amputations.

Endothelial cells modulate several vascular functions and represent an important target for prevention and treatment of diabetes-induced vascular complications (Kolluru et al., 2012). In fact, endothelial dysfunction, which manifests itself by decreased bioavailability of endothelium-derived nitric oxide (NO), and endothelial cell activation, characterized by increased expression of cell-surface adhesion molecules, are defining features of vascular pathologies (Rask-Madsen and King, 2007). Moreover, endothelial cells are the main cells involved in the formation of new blood vessels from pre-existing ones, a process termed angiogenesis, and the abnormalities in this process also contribute to the development of vascular complications (Antonetti et al., 2012; Falanga, 2005; Zent and Pozzi, 2007). While deficient angiogenesis is associated with critical limb ischemia (Falanga, 2005), excessive angiogenesis is implicated in the pathogenesis of retinopathy (Antonetti et al., 2012) and nephropathy (Zent and Pozzi, 2007).

The insulin-sensitizing thiazolidinedione (TZD) drugs are agonists of the peroxisome proliferator-activated receptor-γ (PPARγ),

* Correspondence to: Avenida Professor Lineu Prestes 580, Cidade Universitária, São Paulo, SP, Brazil.
E-mail addresses: dspa@usp.br, dspabdalla@gmail.com (D.S.P. Abdalla).

http://dx.doi.org/10.1016/j.ejphar.2016.04.038
0014-2999/

a ligand-activated transcription factor of the nuclear hormone receptor superfamily – and are used clinically for the treatment of type 2 diabetes. PPARγ is a master regulator of energy homeostasis, and in addition to its role in adipogenesis, strong evidence supports that PPARγ activation also regulates endothelial biology (Bishop-Bailey and Swales, 2008). Consistently, TZDs affect endothelial cell functions and activation. For instance, TZDs enhance NO production in endothelial cells (Calnek et al., 2003; Polikandriotis et al., 2005), suppress gene expression of adhesion molecules, such as vascular cell adhesion molecule 1 (VCAM-1), intercellular adhesion molecule 1 (ICAM-1) and E-selectin (Kurebayashi et al., 2005; Pasceri et al., 2000; Wang et al., 2002), and inhibit the production of reactive oxygen species (ROS) (Ceolotto et al., 2007; Fujisawa et al., 2009). Furthermore, TZDs also regulate angiogenesis in both *in vitro* and *in vivo* models (Biscetti et al., 2008; Panigrahy et al., 2002; Scoditti et al., 2010; Xin et al., 1999). Nevertheless, despite the beneficial effects of TZDs on endothelial cells homeostasis, these drugs had restricted prescription or have been withdrawn from the market because of their association with important adverse effects, including weight gain, liver injury, and increased risk to bone fracture and heart failure (Cariou et al., 2012). Such safety concerns have highlighted the need to identify and characterize new drug candidates from the TZD class of drugs. In the current study, we sought to investigate the effects of three new TZDs on endothelial cells, with a special emphasis on the production of NO and ROS, gene expression of adhesion molecules, and modulation of cell migration and tube formation and compare the results to those obtained with rosiglitazone (RSG), which was used as a TZD control.

2. Materials and methods

2.1. Chemicals and reagents

The compounds GQ-32 [3-biphenyl-4-ylmethyl-5-(4-nitro-benzylidene)-thiazolidine-2,4-dione], GQ-169 [5-(4-chloro-benzylidene)-3-(2,6-dichloro-benzyl)-thiazolidine-2,4-dione], and LYSO-7 [5-(5-bromo-1*H*-indol-3-ylmethylene)-3-(4-chlorobenzyl)-thiazolidine-2,4-dione] (Fig. 1) were synthesized in the Laboratory of Design and Drug Synthesis of the Federal University of Pernambuco (Recife, Pernambuco, Brazil). Rosiglitazone (RSG) was purchased from Cayman Chemicals (Ann Arbor, MI, USA). Tumor necrosis factor α (TNF-α) was obtained from Sigma-Aldrich (St. Louis, MO, USA). 4-Amino-5-methylamino-2′,7′-difluorofluorescein diacetate (DAF-FM diacetate) and 5-(and-6) chloromethyl-2′,7′ dichlorodihydrofluorescein diacetate acetyl ester (CM-H_2DCFDA) were obtained from Molecular Probes Inc. (Eugene, OR, USA). Tissue culture media, serum, and supplements were purchased from Life Technologies (Carlsbad, CA, USA) unless otherwise stated.

2.2. GQ-32, GQ-169, and LYSO-7 synthesis

Thiazolidine-2,4-dione was N-(3)-alkylated in the presence of sodium hydroxide, which allows the thiazolidine sodium salt to react with the benzyl halide in a hot ethanol medium, yielding the first group of intermediates. The 5-arylidene-3-benzyl-thiazolidine-2,4-diones were prepared by a nucleophilic Michael addition of the 3-benzyl-thiazolidine-2,4-dione and the respective aryl-substituted ethyl-(2-cyano-3-phenyl)-acrylates to obtain the arylidene-thiazolidine-2,4-diones 3-substituted. After cooling, the precipitates were purified by column chromatography or crystallized in suitable solvents. The ethyl-(2-cyano-3-phenyl)-acrylates were prepared by Knoevenagel condensation of ethyl cyanoacetic ester and substituted benzaldehydes in the presence of piperidine (Pitta et al., 2007). All of the synthesized compounds were analyzed with multiple analytical procedures. Melting points were determined in a capillary tube using a Quimis apparatus. Infrared spectra (IR) were recorded on a Bruker IFS66 spectrometer (Bruker Daltronics, Billerica, MA, USA). ^{1}H NMR spectra were recorded on a Varian Plus 300 MHz spectrometer using dimethyl sulfoxide (DMSO)-d_6 as a solvent and tetramethylsilane as an internal standard. Mass spectra were recorded by a high capacity ion trap mass spectrometer (HCT Ultra; Bruker Daltonics, Billerica, MA, USA) and were performed by electrospray ionization in negative mode or by electronic impact. The following results were obtained: GQ-32—$C_{23}H_{16}N_2O_4S$. Mp: 152–153 °C. Yield: 52%. IR (KBr, cm^{-1}): 1738, 1691, 1614, 1410, 1343, 1149, 843. ^{1}H NMR (300 MHz, DMSO-d_6) δ 8.36 (d, 2*H*, J=9.0 Hz, 5-Ar-H, 3,5 pos.), 8.09 (s, 1*H*,=CH), 7.91 (d, 2*H*, J=9.0 Hz, 5-Ar-H, 2,6 pos.), 7.66–7.62 (m, 4*H*, 3-Ar-H, 3,5 pos. and 2′,6′ pos.), 7.48–7.33 (m, 5*H*, 3-Ar-H, 2,6 pos. and 3′,4′,5′ pos.). MS *m/z* (%), observed: 167 (100.0), 416 (77.3), 32 (73.8), calculated 416.08; GQ-169–$C_{17}H_{10}Cl_3NO_2S$. Mp: 208–210 °C. Yield: 57%. IR (KBr, cm^{-1}): 1744, 1686, 1611, 1488, 1438, 1378, 1339, 1138, 1075, 939, 783, 568, 521. ^{1}H NMR (300 MHz, DMSO-d_6) δ 7.91 (s, 1*H*,=CH), 7.62 (d, 4*H*, J=2.1 Hz, 5-Ar-H, 2,3,5,6 pos.), 7.50–7.47 (m, 2*H*, 3-Ar-H, 3,5 pos.), 7.37 (t, 1*H*, J=16.2 Hz, J=7.2 Hz, 3-Ar-H, 4 pos.), 5.09 (s, 2*H*,-CH_2). MS *m/z* [M−H], observed: 397.04, calculated 398.69. The analytical results of LYSO-7 have already been reported (Santin et al., 2013b).

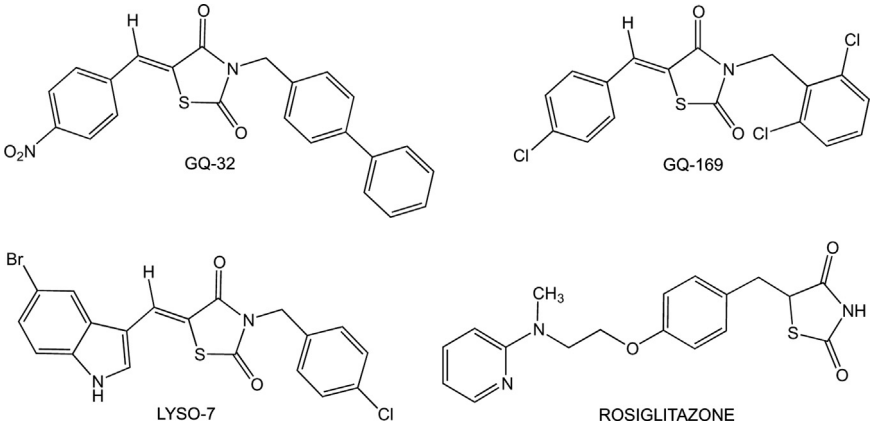

Fig. 1. Chemical structures of GQ-32, GQ-169, LYSO-7, and rosiglitazone. GQ-32 [3-biphenyl-4-ylmethyl-5-(4-nitro-benzylidene)-thiazolidine-2,4-dione], GQ-169 [5-(4-chloro-benzylidene)-3-(2,6-dichloro-benzyl)-thiazolidine-2,4-dione], and LYSO-7 [5-(5-bromo-1*H*-indol-3-ylmethylene)-3-(4-chlorobenzyl)-thiazolidine-2,4-dione] were synthesized as indicated under Materials and Methods.

2.3. Cell culture

Human umbilical vein endothelial cells (HUVECs) were maintained in RPMI 1640 medium, and human embryonic kidney 293 cells (HEK293) were cultured in high-glucose Dulbecco's modified Eagle's medium (DMEM). Media were supplemented with 10% fetal bovine serum (FBS), 2 mM L-glutamine, 100 μg/ml streptomycin, and 100 IU/ml penicillin. Cells were incubated at 37 °C with 5% CO_2 and stimulated with GQ-32, GQ-169, and LYSO-7 in medium containing 1% FBS. Control cells were treated with vehicle, DMSO, at concentrations used for the TZDs ($<0.1\%$ vol/vol).

2.4. Cell viability assays

To assess the new TZDs effects on cell viability, a 3-(4,5-dimethylthiazol-2yl)-2,5-diphenol-2*H*-tetrazolium bromide (MTT) reduction assay was conducted (Denizot and Lang, 1986). In brief, HUVECs were seeded in a 96-well tissue culture plates (5×10^3 cells/well) and treated with 0.625, 1.25, 2.5, 5, or 10 μM GQ-32, GQ-169, LYSO-7, or RSG for 24 h. The cells then were incubated with MTT (1 mg/ml) at 37 °C for 3 h and lysed in 100 μl DMSO. The absorbance was evaluated at 570 nm using a Synergy MX plate reader (BioTek, Winooski, VT, USA). To study the effects of new TZDs on cell death, HUVECs were treated with 5 μM GQ-32, GQ-169, LYSO-7, or RSG for 24 h, and samples were analyzed by flow cytometry with Canto II (Becton Dickinson, Franklin Lakes, NJ, USA) using annexin V-FITC apoptosis detection kit (Sigma-Aldrich, St. Louis, MO, USA), according to the manufacturer's instructions.

2.5. Transient transfection and reporter gene assay

The pCMX expression plasmids for PPARγ and the minimal promoters containing multiple binding sites for the PPAR-response element (UAS-LUC) were kindly provided by Dr. A. Castrillo (Instituto de Investigaciones Biomédicas Alberto Sols). In brief, HEK293 cells seeded in 48-well plates (5×10^4 cells/well) were transiently transfected using Lipofectamine 2000 reagent (Life Technologies, Carlsbad, CA, USA) according to the manufacturer's instructions. Eight hours after transfection, cells were treated with vehicle, GQ-32, GQ-169, LYSO-7, or RSG and further incubated for 16 h. Reporter activities were assayed using the dual luciferase/renilla assay system following the recommendations of the supplier (Promega, Madison, WI, USA). Green fluorescent protein was used as a control for transfection efficiency.

2.6. Measurement of intracellular ROS

To determine the effect of new TZDs on oxidative stress, the intracellular formation of ROS was detected using the ROS-sensitive fluorescent probe CM-H_2DCFDA as described previously (Fujisawa et al., 2009). Cells were incubated in RPMI 1640 medium with 5.6 or 30 mM glucose plus 5 μM GQ-32, GQ-169, LYSO-7, or RSG. The cells then were washed, and intracellular ROS formation was assayed by CM-H_2DCFDA oxidation-based fluorescence. Fluorescence was measured in a Synergy MX plate reader (BioTek, Winooski, VT, USA).

2.7. Measurement of intracellular NO production and release

Intracellular NO measurement was performed as described previously using the NO-specific fluorescence probe DAF-FM diacetate. In brief, HUVECs were incubated in RPMI 1640 medium containing 5 μM DAF-FM diacetate for 45 min at 37 °C in the dark. After loading, cells were rinsed three times with PBS to remove excess probe and then incubated for an additional 30 min with fresh medium to allow complete de-esterification of the intracellular diacetates, after which 5 μM of either GQ-32, GQ-169, LYSO-7, or RSG was added to the wells. Fluorescence (emission wavelength, 485 nm; excitation wavelength, 535 nm) was measured temporally at 37 °C from 0 to 4 h using the bottom-reading mode in a Synergy MX plate reader (BioTek, Winooski, VT, USA).

The NO concentration in the culture medium was evaluated by measuring the NO_2^- accumulation with a nitric oxide analyzer (NOA™ 280; Sievers Inc., Boulder, CO, USA) as described previously (Bonini et al., 2002). In brief, HUVECs were grown to confluence in six-well plates and then incubated with or without 5 μM GQ-32, GQ-169, LYSO-7, or RSG for 24 h, and 100 μl of culture supernatants were injected into a reflux chamber containing vanadium(III) in 3 N HCl heated to 90 °C. The NO produced was detected by gas phase chemiluminescence after reaction with ozone. A calibration curve then was created using a sodium nitrate standard solution.

2.8. Migration assay

Endothelial cell migration was analyzed using an *in vitro* scratch assay as described previously (Liang et al., 2007). In brief, *in vitro* scratched wounds were created by scraping the endothelial confluent monolayers with a sterile tip. After injury of the monolayer, the cells were washed gently and incubated for 24 h with RPMI 1640, 1% FBS containing 5 μM GQ-32, GQ-169, LYSO-7, or RSG. Immediately after wounding and at the end of the experiment, the wound areas were photographed. The AxioVision 4.0 software (Carl Zeiss Inc., Jena, Germany) was used to determine the extent of migration by determining the uncovered area in three distinct microscopic fields, representative of each culture condition. Each experiment was performed in triplicate and repeated three times.

2.9. Matrigel assay

HUVECs (1×10^5/well) were plated on Matrigel (BD Biosciences, Mountain View, CA) and allowed to adhere for 2 h at 37 °C. GQ-32, GQ-169, LYSO-7, or RSG then was added at 5 μM. Digital photographs of the cells were collected using a Nikon Eclipse TS100 microscope (Nikon Ltd., London, United Kingdom). Each experiment was performed in triplicate, and five random pictures were taken of each well at a magnification of $\times 10$. The tube formation was quantified using U.S. National Institutes of Health ImageJ program (Carpentier, 2012). Mean values of total length in each sample were used to represent the tube formation.

2.10. Assessment of anti-inflammatory activity

For the evaluation of the new TZDs effects on the adhesion molecules expression, HUVECs were incubated with new TZDs (5 μM) for 4 h in the absence or presence of TNF-α (10 ng/ml). The gene expression of VCAM-1, ICAM, and E-selectin mRNAs were analyzed by real-time polymerase chain reaction (PCR).

2.11. Quantitative real-time PCR analysis

Total RNA was isolated with Trizol (Life Technologies, Carlsbad, CA, USA), and 2 μg RNA was reverse transcribed into cDNA by SuperScript VILO cDNA synthesis kit (Life Technologies). Quantitative real-time PCR was performed in an ABI Prism 7500 Fast Sequence Detector (Applied Biosystems, Foster City, CA, USA) using SYBR Green PCR Master Mix (Applied Biosystems) and specific primer pairs listed in Table 1. The cycling program was 95 °C for 10 min followed by 40 cycles of 95 °C for 15 s and 60 °C for 60 s Each sample was run in triplicate. Expression of each target gene was normalized to 18S rRNA relative expression as an internal

Table 1
Forward and reverse primers used for real-time PCR.

Gene	Forward primer	Reverse primer
E-selectin	5′-CTCTGACAGAAGAAGCCAAGAAC-3′	5′-GCTGTGTAGCATAGGGCAAG-3′
bFGF	5′-TGTGCTAACCGTTACCTGGCT-3′	5′-CAGTGCCACATACCAACTG-3′
ICAM-1	5′-CTTCTCCTGCTCTGCAACCC-3′	5′-GGGAGAGCACATTCACGGTC-3′
IL-8	5′-TGTGTGAAGGTGCAGTTTTG-3′	5′-ATTTCTGTGTTGGCGCAGT-3′
NOS3	5′-GTGGCTGTCTGCATGGACCT-3′	5′-CCACGATGGTGACTTTGGCT-3′
PDGFB	5′-TTCCCGAGGAGCTTTATGAG-3′	5′-GGGTCATGTTCAGGTCCAA-3′
TGFβ	5′-TCGCCAGAGTGGTTATCTTTT-3′	5′-TAGTGAACCCGTTGATGTCC-3′
TSP-1	5′-CTTCAAGCCAGAGGCCTACG-3′	5′-CCGCCTCTGTCTTCTTCAGC-3′
VCAM-1	5′-CTGGAAATGCAACTCTCACC-3′	5′-GTCTCCAATCTGAGCAGCAA-3′
VEGFA	5′-ATCTTCAAGCCATCCTGTGTGC-3′	5′-CAAGGCCCACAGGGATTTTC-3′
18S rRNA	5′-GTAACCCGTTGAACCCCATT-3′	5′-CCATCCAATCGGTAGTAGCG-3′

efficiency control. The mRNA fold change was calculated using the $2^{-\Delta\Delta C(t)}$ method, with the values expressed as fold increases relative to the untreated control (Livak and Schmittgen, 2001).

2.12. Data analysis

All results are expressed as the mean ± S.D. from triplicate measurements performed in at least two independent experiments. Statistical analysis was performed by one-way ANOVA followed by Dunnett's test. Probability values were considered significant at $P < 0.05$.

3. Results

3.1. New TZDs show low cytotoxicity on endothelial cells and are weak PPARγ agonists

To determine the cytotoxicity of new TZDs, HUVEC were treated with vehicle (0.01% DMSO) or various concentrations (0.625–10 μM) of new TZDs for 24 h, and cell viability was analyzed by MTT assay. As shown in Fig. 2A, similar to RSG, new TZDs show low cytotoxicity on HUVEC. However, GQ-32 and GQ-169 induced a significant decrease in cell viability at 10 μM. In contrast, treatment with LYSO-7 did not alter the overall viability of the cells compared with cells treated with vehicle.

Although a decrease of cell viability was also detected with GQ-32 and GQ-169 at 5 μM, no morphological alterations of the cellular surface were observed. Therefore, to further confirm 5 μM as a nontoxic concentration, we evaluated the effects of new TZDs on cell death. HUVECs were then incubated with new TZDs or RSG for 24 h, and cell death was determined with annexin V/PI staining by flow cytometry evaluating four different populations: viable cells (annexin V^-/PI^-), nonviable cells (annexin V^-/PI^+), and early-stage (annexin V^+/PI^-) and late-stage (annexin V^+/PI^+) apoptosis. No significant effect was observed in cell populations when HUVECs were incubated with new TZDs or RSG for 24 h, suggesting 5 μM as a nontoxic concentration (Fig. 2B). Hence, 5 μM was the elected concentration for the following experiments.

Since PPARγ is the main molecular target of TZDs, such as RSG and pioglitazone, we examined whether the new TZDs might act as agonists of PPARγ using a reporter gene assay. As illustrated in Fig. 2C, new TZDs induce PPARγ activation. However, in contrast to the full PPARγ agonist RSG, only a weak activation of PPARγ was observed with new TZDs. Indeed, relative to full PPARγ activation induced by RSG, the detected activation with new TZDs was approximately 20–25%, suggesting that these compounds might act as partial agonists of PPARγ.

3.2. New TZDs reduce ROS production and increase intracellular levels of nitric oxide in HUVEC

To evaluate the effects of new TZDs on oxidative stress in HUVEC, cells were incubated in normal and high-glucose medium, co-treated with new TZDs or RSG for 24 h, and the intracellular ROS production was examined using the probe CM-H_2DCFDA. As shown in Fig. 3A, a significant increase in CM-H_2DCFDA-associated fluorescence was observed in the cells incubated with 30 mM glucose compared with 5.6 mM glucose medium. On the other hand, the treatment with RSG, GQ-169, and LYSO-7 inhibited the glucose-induced ROS production, whereas GQ-32 did not affect intracellular ROS production in cells incubated with 30 mM glucose. In addition, when HUVECs were incubated in normal glucose condition (5.6 mM), neither RSG nor new TZDs affected ROS production (Supplementary Data).

The effects of new TZDs were also explored on production and release of nitric oxide in HUVEC. As depicted in Fig. 3B, new TZDs significantly increased intracellular levels of NO after 4 h

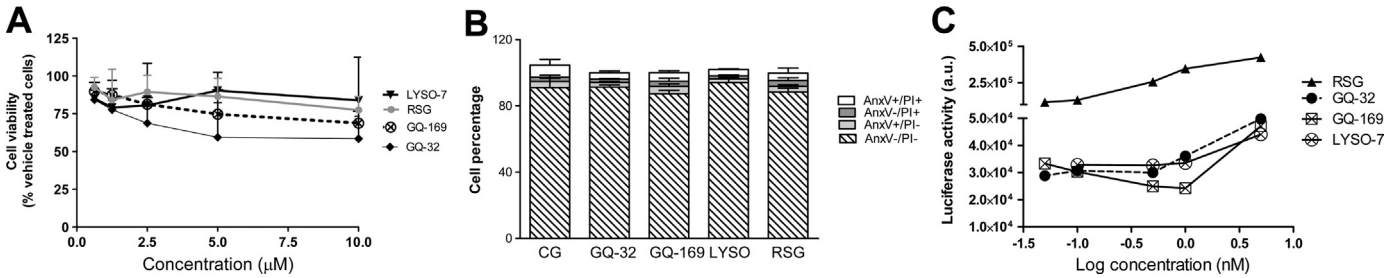

Fig. 2. New TZDs show low cytotoxicity in HUVECs and act as partial agonists of PPARγ. (A) The effects of new TZDs on cell viability were measured by MTT assay. HUVECs were incubated with increasing concentrations of GQ-32, GQ-169, LYSO-7, or RSG for 24 h and then analyzed as indicated. Data are expressed as percentage of vehicle (0.01% DMSO)-treated control culture conditions. $N=8$ from three independent experiments. (B) Effects of new TZDs on endothelial cell death were determined with annexin/PI staining by flow cytometry after incubation of HUVECs with new TZDs or RSG (at 5 μM) for 24 h. $N=6$ from two independent experiments. (C) Cellular activation of PPARγ was determined with a reporter gene assay. Human embryonic kidney 293 cells were transiently transfected with specific plasmids and treated with increasing concentrations of GQ-32, GQ-169, LYSO-7, or RSG for 16 h. Transcriptional responses were evaluated using a luciferase reporter gene assay kit. $N=6$ from two independent experiments. Data are expressed as mean ± S.D. $^*P < 0.05$ *vs.* control group.

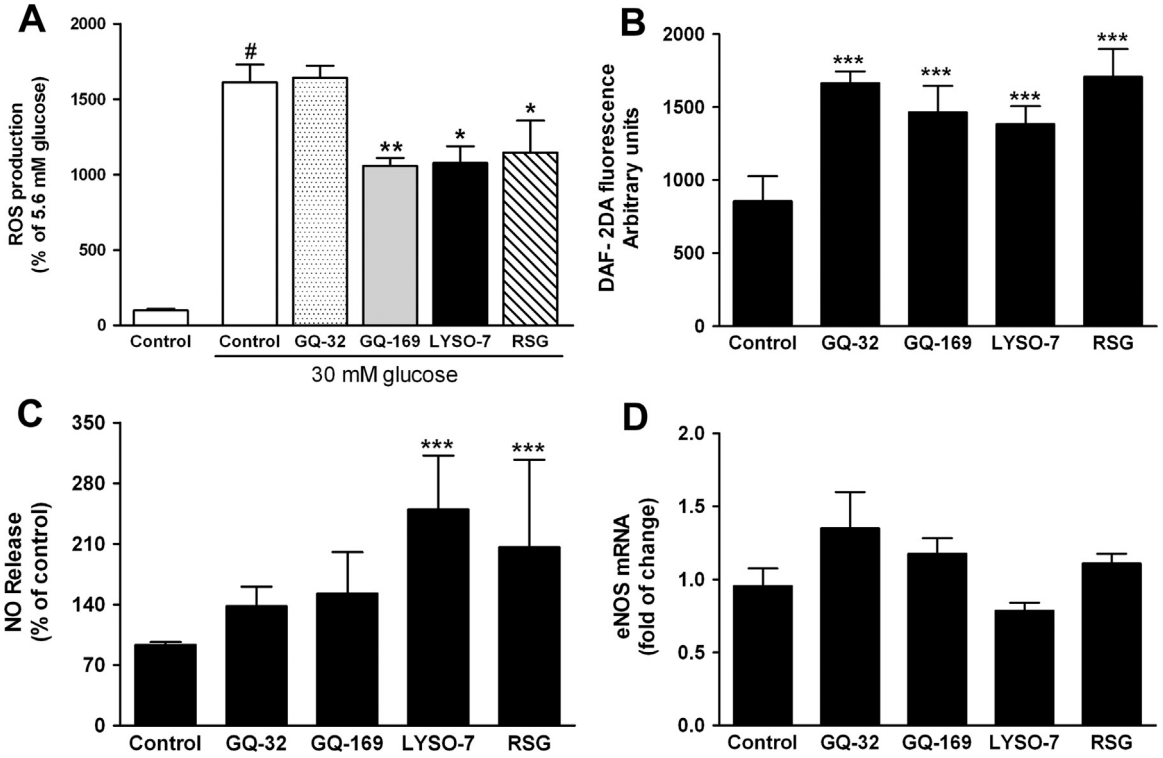

Fig. 3. New TZDs affect ROS and NO production in HUVECs. (A) Quantification of effects of new TZDs on ROS intracellular levels relative to control group. HUVECs were incubated with RPMI 1640 medium (5.6 mM glucose or 30 mM glucose) plus a 5 μM concentration of new TZDs or RSG, and ROS intracellular levels were measured using the probe CM-H_2DCFDA. (B–C) New TZDs affect intracellular levels (B) and release (C) of NO. (B) HUVECs were incubated with new TZDs or RSG (at 5 μM) for 4 h, and intracellular levels of NO were determined with NO-specific fluorescence probe DAF-FM. (C) Quantification of NO release relative to control group. NO release was measured with chemiluminescence analysis of culture medium after treatment with new TZDs or RSG (at 5 μM) for 24 h. (D) HUVEC eNOS expression after treatment with new TZDs or RSG for 4 h. The mRNA levels of eNOS were explored by real-time PCR. Data are expressed as mean ± S.D. of three independent experiments performed at least in triplicate. $^{*}P < 0.05$,$^{**}P < 0.01$,$^{***}P < 0.001$ *vs.* control group, $\#P < 0.001$ *vs.* control group incubated with 5.6 mM glucose medium.

incubation. Furthermore, NO release was augmented when HUVECs were treated with LYSO-7 or RSG for 24 h (Fig. 3C). On the other hand, treatments with 5 μM GQ-32 and GQ-169 were unable to affect NO release (Fig. 3C). In addition, to determine whether new TZDs regulate NO production through modulation of endothelial nitric oxide synthase (eNOS) expression, HUVECs were treated for 4 h, and mRNA levels of eNOS were determined with real-time PCR. As can be observed in Fig. 3D, eNOS mRNA expression was not affected by new TZDs or RSG.

3.3. New TZDs down-regulate TNF-α-induced expression of adhesion molecules in HUVECs

To evaluate the effects of new TZDs on endothelial cell activation, HUVECs were incubated with new TZDs for 4 h in the absence or presence of 10 ng/ml TNF-α. As shown in Fig. 4, the mRNA levels of proinflammatory adhesion molecules VCAM-1, ICAM-1, and E-selectin were remarkably up-regulated in response to TNF-α. As expected, RSG significantly attenuated the TNF-α-induced expression of VCAM-1, ICAM-1, and E-selectin. Similar to RSG, treatment with 5 μM GQ-32, GQ-169, and LYSO-7 suppressed the induction of VCAM-1 and ICAM-1 stimulated by TNF-α. In contrast, the TNF-α-induced expression of E-selectin was unaffected by the new TZDs (Fig. 4).

3.4. New TZDs affect endothelial cell migration and tube formation in vitro

We next tested whether new TZDs would also affect biological processes involved in angiogenesis. Because migration of endothelial cells is crucial during angiogenesis, we explored the impact of new TZDs on migration in HUVECs using the *in vitro* wound scratch assay. As demonstrated in Fig. 5A, GQ-32 and GQ-169 significantly induced endothelial cell migration, whereas no effect was observed with LYSO-7 treatment. It is noteworthy that, under our experimental conditions, 5 μM RSG reduced endothelial cell migration by 16%, but this was not statistically significant (Fig. 5B).

To further verify that new TZDs would also affect endothelial capacity to form capillary-like structures, an *in vitro* tube formation assay was performed using Matrigel basement membrane matrix, which mimics capillary formation *in vivo*. As illustrated in Fig. 5C, RSG suppressed the formation of tube-like structures. In contrast, LYSO-7 did not affect tube formation, whereas GQ-32 and GQ-169 stimulated the formation of tube-like structures (Fig. 5C-D).

To understand the cellular and molecular mechanisms through which new TZDs affected cell migration and tube formation of endothelial cells, we evaluated the effects of new TZDs on gene expression of angiogenic molecules. Consistent with increased cell migration and formation of tube-like structures, GQ-32 and GQ-169 induced vascular endothelial growth factor A (VEGFA) expression (Fig. 6A). The treatment with GQ-169 also up-regulated the mRNA levels of basic fibroblast growth factor (bFGF, Fig. 6B) and interleukin 8 (CXCL8, Fig. 6C) and did not affect transforming growth factor β (TGFβ (Fig. 6D)). expression. In turn, GQ-32 induced expression of TGFβ (Fig. 6D) and CXCL8 (Fig. 6C) but did not influence mRNA bFGF levels (Fig. 6B). RSG inhibited VEGFA mRNA expression, and LYSO-7 down-regulated platelet-derived growth factor (PDGF)-BB mRNA levels (Fig. 6E). Both LYSO-7 and RSG also decreased the expression of TGFβ mRNA (Fig. 6D). The expression of thrombospondin-1, a potent inhibitor of angiogenesis, was not

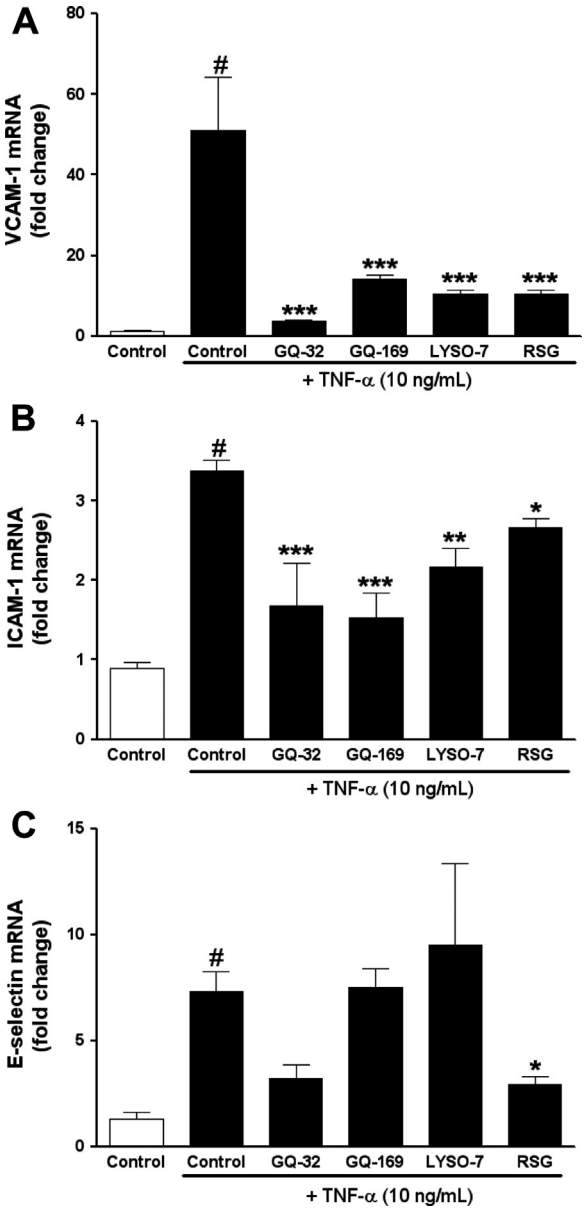

Fig. 4. Effects of new TZDs on mRNA levels of adhesion molecules. HUVECs were incubated with new TZDs or RSG at 5 μM and cotreated with TNF-α (10 ng/ml) for 4 h. The mRNA levels of VCAM-1 (A), ICAM-1 (B), and E-selectin (C) were explored by real-time PCR. Data are expressed as mean ± S.D. of three independent experiments performed in triplicate. $^{\#}P < 0.001$ *vs.* control group without TNF-α,$^{*}P < 0.05$, $^{**}P < 0.01$,$^{***}P < 0.001$ *vs.* control group with TNF-α.

changed either by RSG or by new TZDs (Fig. 6F).

4. Discussion

In this study, we report that three new TZDs, namely GQ-32, GQ-169, and LYSO-7 affect endothelial cell functions and activation. We show that the new TZDs act as partial agonists of PPARγ, inhibit ROS production and adhesion molecules expression, and influence NO production. We further reveal that GQ-32 and GQ-169 also stimulate endothelial cell migration and tube formation *in vitro*. Interestingly, compared with RSG, LYSO-7 demonstrates equivalent properties on HUVEC, whereas the evidence presented here supports that GQ-32 and GQ-169 possess similar anti-inflammatory properties, but distinct effects on angiogenesis.

Endothelium-derived NO is a signaling molecule relevant to vascular homeostasis and modulates the vascular tone, endothelial cell growth, adhesion of platelet and leukocytes, platelet aggregation (Lundberg et al., 2015) and angiogenesis (Ridnour et al., 2005). It is noteworthy that reduced bioavailability of NO, the main feature of endothelial dysfunction, is associated with the pathogenesis of vascular complications and that strategies to increase NO signaling have been extensively explored. Corroborating results from previous studies (Calnek et al., 2003; Polikandriotis et al., 2005), we show that RSG increases the production and release of NO without affecting eNOS expression. LYSO-7 demonstrates a similar effect compared with RSG. However, GQ-32 and GQ-169 display only a weak and transient effect on NO production as both treatments failed to modify the release of NO from HUVEC measured by chemiluminescence analysis of culture media.

Accumulating evidence indicates that increased ROS production also may influence endothelial cell function and plays a crucial role in the development of vascular pathologies (Schaffer et al., 2012). In this respect, previous studies propose that antioxidant agents contribute to the prevention of vascular complications. Of note, the suppression of glucose-induced ROS production is described as a beneficial effect of TZDs class of drugs (Fujisawa et al., 2009). Therefore, we hypothesized that the new TZDs could affect glucose-induced ROS production. Our results show that only GQ-169 and LYSO-7 reduced glucose-induced ROS production whereas GQ-32 failed to show an effect on ROS production in endothelial cells under our experimental conditions.

TZD class of drugs also presents anti-inflammatory properties not only in endothelial cells but also in different cell types and animal models (Pasceri et al., 2000; Santin et al., 2013a; Wang et al., 2002). The anti-inflammatory effects of TZDs have been suggested to be mediated through suppression of adhesion molecules expression (Pasceri et al., 2000; Wang et al., 2002), which regulate the recruitment and binding of circulating leukocytes to the vessel wall and are essential in inflammatory responses (Golias et al., 2007). As expected, in our study, RSG inhibited the expression of VCAM-1, ICAM-1, and E-selectin in response to TNF-α. Interestingly, although GQ-32, GQ-169, and LYSO-7 have poor agonist activities on PPARγ compared to RSG, they show equivalent inhibition of TNF-α-induced expression of VCAM-1 and ICAM-1, suggesting that the inhibitory effects on endothelial cell activation of these new TZDs may be PPARγ independent. In fact, previous studies employing PPARγ null cells, demonstrate that PPARγ is not essential for the anti-inflammatory effects of TZDs (Chawla et al., 2001; Feinstein et al., 2005). Our results are also in agreement with recent data describing the anti-inflammatory effects of LYSO-7. LYSO-7 has been also shown as a cyclooxygenase inhibitor, and its anti-inflammatory effects have been already established in neutrophils (Santin et al., 2013b) and macrophages, as well as in a mouse model of atherosclerosis (Cesar et al., 2015).

Previous studies exploring the effects of TZDs on angiogenesis have shown controversial results. Evidence from *in vitro* and *in vivo* models indicate that, through PPARγ activation, TZDs might demonstrate antiangiogenic effects (Aljada et al., 2008; Panigrahy et al., 2002; Xin et al., 1999), but also promote angiogenesis, which was associated with eNOS activation and resulted in enhanced neovascularization (Biscetti et al., 2008; Chu et al., 2006; Gealekman et al., 2008; Nagahama et al., 2012). Discrepancies between these results probably rely on study design, PPAR affinity/activation and PPARγ-independent actions of TZDs. Under our experimental conditions, the new TZDs, GQ-32 and GQ-169, stimulate two hallmarks of angiogenesis, endothelial cell migration and their differentiation into tube-like structures. By contrast, in line with previous studies, we also showed that RSG inhibited the endothelial tube formation under our experimental conditions, strengthening the antiangiogenic action associated with this TZD.

A major limitation of our study is that the underlying

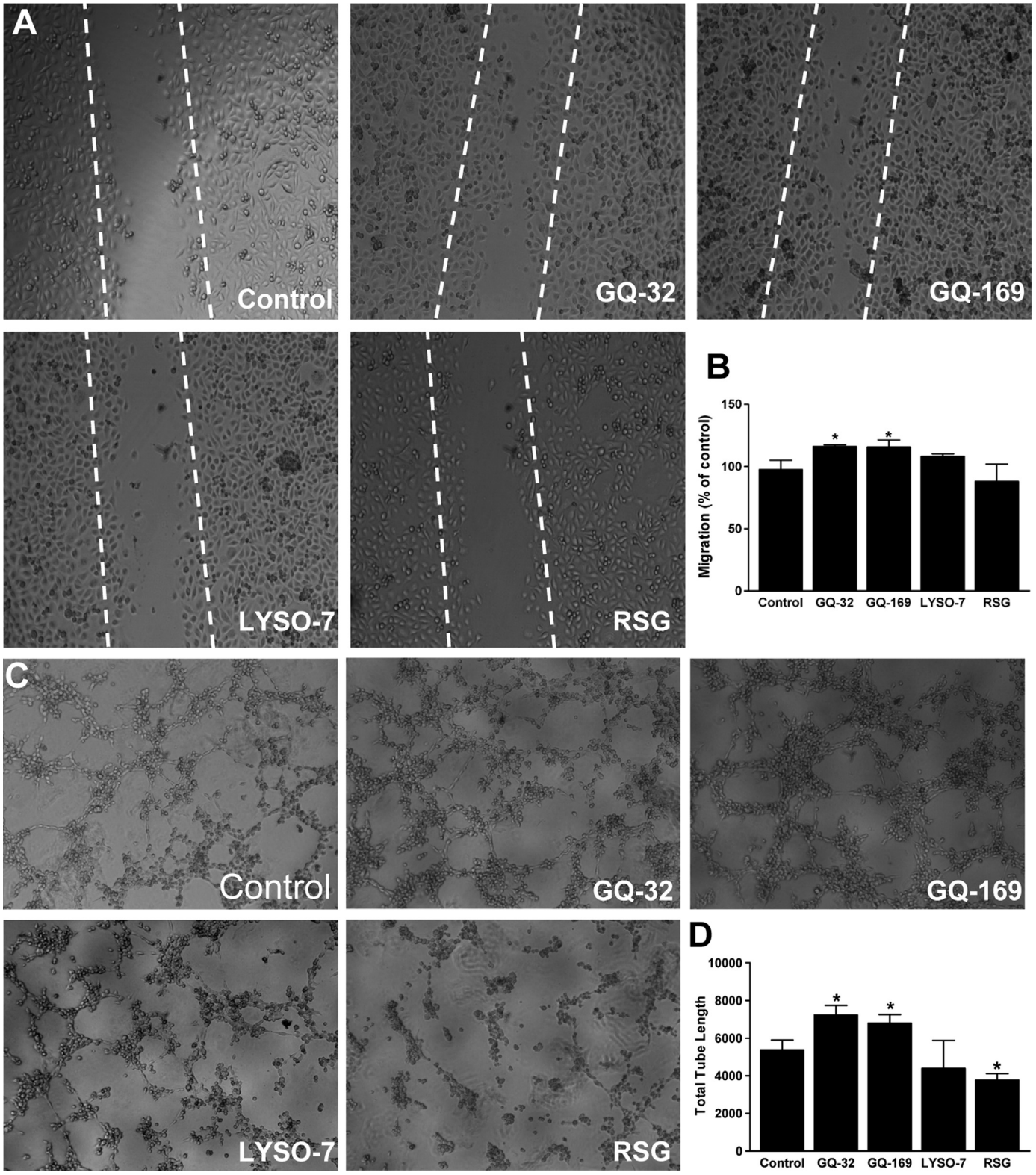

Fig. 5. Effects of new TZDs on angiogenesis. (A) A cell-free area was introduced with a pipette tip in HUVEC confluent monolayers, and cells were incubated with RPMI 1640, 1% FBS containing 5 μM GQ-32, GQ-169, LYSO-7, or RSG for 24 h. Representative pictures show cell migration after 24 h of treatment. Dashed lines indicate the initial scratch margins. (B) Quantification of HUVEC migration relative to control group. Data are expressed as mean ± S.D. $^{*}P < 0.05$ *vs.* control group. (C) Tube formation of HUVECs using Matrigel basement membrane matrix. Representative photographs after 6-h treatment with new TZDs and RSG. (D) Graphical representation of tube formation. Total tube length as calculated by the ImageJ angiogenesis analyzer. Data are expressed as mean ± S.D. $^{*}P < 0.05$ *vs.* control group.

mechanisms responsible for the proangiogenic effects of GQ-32 and GQ-169 were not completely elucidated. However, since angiogenesis is regulated by the balance of proangiogenic and anti-angiogenic molecules (Carmeliet and Jain, 2011), we speculate that the enhanced expression of proangiogenic molecules might contribute to the effects of new TZDs on angiogenesis. Our results reveal that GQ-32 and GQ-169 increased the mRNA levels of VEGFA in HUVEC, whereas an opposite effect was observed with

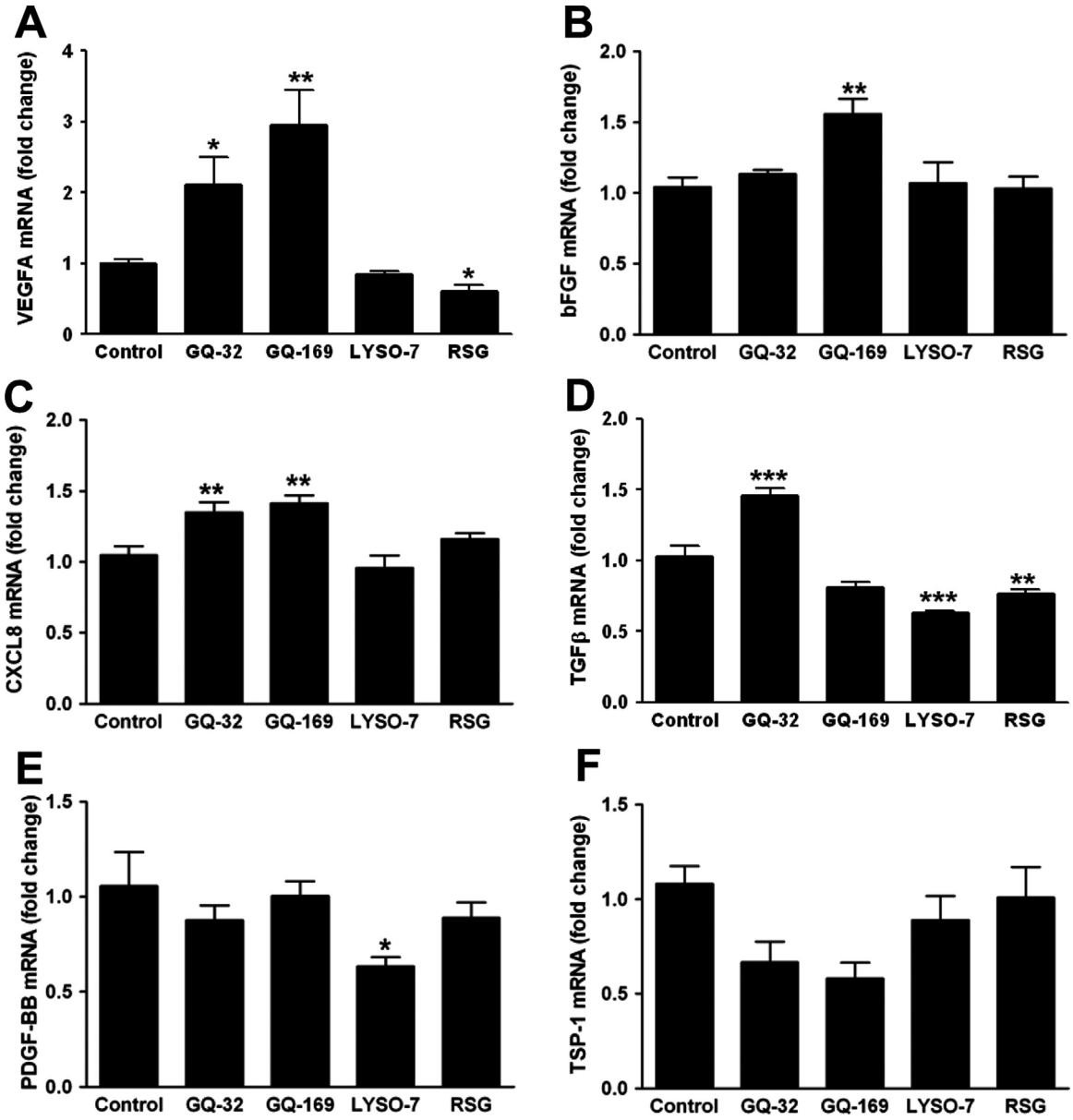

Fig. 6. Effects of new TZDs on mRNA levels of angiogenic molecules. HUVECs were incubated with new TZDs or RSG at 5 μM for 4 h, and the mRNA levels of VEGFA (A), bFGF (B), CXCL8 (C), TGFβ (D), PDGF-BB (E), and thrombospondin-1 (TSP-1, F) were explored by real-time PCR. Data are expressed as mean ± S.D. of three independent experiments performed in triplicate. $^{*}P < 0.05$,$^{**}P < 0.01$,$^{***}P < 0.001$ *vs.* control group.

RSG. VEGFA is the major modulator of angiogenesis and is involved in the regulation of endothelial cell proliferation, survival, and migration (Koch and Claesson-Welsh, 2012). CXCL8, bFGF, PDGF-BB, and TGFβ are also described as relevant molecular players involved in angiogenesis (Carmeliet and Jain, 2011). The evidence demonstrates that bFGF and CXCL8 modulate endothelial cell migration and capillary tube formation (Li et al., 2005) and PDGF-BB and TGFβ contribute to the vessel maturation (Carmeliet and Jain, 2011; Pardali et al., 2010). In our study, although both GQ-32 and GQ-169 enhanced CXCL8 expression, only the treatment with GQ-169 up-regulated the mRNA levels of bFGF. GQ-32 also increased the expression of TGFβ, whereas decreased mRNA levels were observed with RSG and LYSO-7. Thus, GQ-32 and GQ-169 induce angiogenesis and increase the gene expression of proangiogenic molecules, thereby revealing that these new TZDs might have different biological actions and activities when compared to full PPARγ agonists.

Taken together, these findings suggest that the new TZDs GQ-32, GQ-169, and LYSO-7 act as partial agonists of PPARγ and show beneficial pleiotropic effects, affecting endothelial cell functions and activation. In addition, the up-regulation of proangiogenic molecules as well as increased cell migration and tube formation observed with GQ-32 and GQ-169 suggest a therapeutic potential in the treatment of clinical conditions associated to impaired angiogenesis, such as ischemic conditions and impaired wound healing.

Conflict of Interest

None declared.

Acknowledgments

This study was supported by São Paulo Research Foundation

(FAPESP Grant 2012/51316-5 to D.S.P.A.) and National Council for Scientific and Technological Development [National Institute of Science and Technology for Pharmaceutical Innovation ((INCT_if/CNPq) Grant 573663/2008-4 to I.R.P.] and CNPq/MICCIN Grant BFU2011-2476 to D.S.P.A. and L.B.G.). R.F. was supported by FAPESP Fellowship 2011/24020-5, and M.R. was supported by fellowships from the FAPESP (2009/53072-3) and the CNPq (151568/2013-8).

Appendix A. Supporting information

Supplementary data associated with this article can be found in the online version at http://dx.doi.org/10.1016/j.ejphar.2016.04.038.

References

Aljada, A., O'Connor, L., Fu, Y.Y., Mousa, S.A., 2008. PPAR gamma ligands, rosiglitazone and pioglitazone, inhibit bFGF- and VEGF-mediated angiogenesis. Angiogenesis 11, 361–367.
Antonetti, D.A., Klein, R., Gardner, T.W., 2012. Diabetic retinopathy. N. Engl. J. Med. 366, 1227–1239.
Biscetti, F., Gaetani, E., Flex, A., Aprahamian, T., Hopkins, T., Straface, G., Pecorini, G., Stigliano, E., Smith, R.C., Angelini, F., Castellot Jr., J.J., Pola, R., 2008. Selective activation of peroxisome proliferator-activated receptor (PPAR)alpha and PPAR gamma induces neoangiogenesis through a vascular endothelial growth factor-dependent mechanism. Diabetes 57, 1394–1404.
Bishop-Bailey, D., Swales, K.E., 2008. The role of PPARs in the endothelium: implications for cancer therapy. PPAR Res. 2008, 904251.
Bonini, M.G., Mason, R.P., Augusto, O., 2002. The mechanism by which 4-hydroxy-2,2,6,6-tetramethylpiperidene-1-oxyl (tempol) diverts peroxynitrite decomposition from nitrating to nitrosating species. Chem. Res. Toxicol. 15, 506–511.
Boulton, A.J., Kirsner, R.S., Vileikyte, L., 2004. Clinical practice. Neuropathic diabetic foot ulcers. N. Engl. J. Med. 351, 48–55.
Calnek, D.S., Mazzella, L., Roser, S., Roman, J., Hart, C.M., 2003. Peroxisome proliferator-activated receptor gamma ligands increase release of nitric oxide from endothelial cells. Arterioscler. Thromb. Vasc. Biol. 23, 52–57.
Cariou, B., Charbonnel, B., Staels, B., 2012. Thiazolidinediones and PPARgamma agonists: time for a reassessment. Trends Endocrinol. Metab. 23, 205–215.
Carmeliet, P., Jain, R.K., 2011. Molecular mechanisms and clinical applications of angiogenesis. Nature 473, 298–307.
Carpentier, G., 2012. ImageJ contribution: Angiogenesis Analyzer. ImageJ News.
Ceolotto, G., Gallo, A., Papparella, I., Franco, L., Murphy, E., Iori, E., Pagnin, E., Fadini, G.P., Albiero, M., Semplicini, A., Avogaro, A., 2007. Rosiglitazone reduces glucose-induced oxidative stress mediated by NAD(P)H oxidase via AMPK-dependent mechanism. Arterioscler. Thromb. Vasc. Biol. 27, 2627–2633.
Cesar, F.A., Rudnicki, M., de Las, H.B., Bosca, L., Lima, M.C., Pitta, I.R., Abdalla, D.S., 2015. New indole-thiazolidine attenuates atherosclerosis in LDLr(-/-) mice. Vasc. Pharmacol. 71, 174–180.
Chawla, A., Barak, Y., Nagy, L., Liao, D., Tontonoz, P., Evans, R.M., 2001. PPAR-gamma dependent and independent effects on macrophage-gene expression in lipid metabolism and inflammation. Nat. Med. 7, 48–52.
Chu, K., Lee, S.T., Koo, J.S., Jung, K.H., Kim, E.H., Sinn, D.I., Kim, J.M., Ko, S.Y., Kim, S.J., Song, E.C., Kim, M., Roh, J.K., 2006. Peroxisome proliferator-activated receptor-gamma-agonist, rosiglitazone, promotes angiogenesis after focal cerebral ischemia. Brain Res. 1093, 208–218.
Denizot, F., Lang, R., 1986. Rapid colorimetric assay for cell growth and survival. Modifications to the tetrazolium dye procedure giving improved sensitivity and reliability. J. Immunol. Methods 89, 271–277.
Falanga, V., 2005. Wound healing and its impairment in the diabetic foot. Lancet 366, 1736–1743.
Feinstein, D.L., Spagnolo, A., Akar, C., Weinberg, G., Murphy, P., Gavrilyuk, V., Dello, R.C., 2005. Receptor-independent actions of PPAR thiazolidinedione agonists: is mitochondrial function the key? Biochem. Pharmacol. 70, 177–188.
Fujisawa, K., Nishikawa, T., Kukidome, D., Imoto, K., Yamashiro, T., Motoshima, H., Matsumura, T., Araki, E., 2009. TZDs reduce mitochondrial ROS production and enhance mitochondrial biogenesis. Biochem. Biophys. Res. Commun. 379, 43–48.
Gealekman, O., Burkart, A., Chouinard, M., Nicoloro, S.M., Straubhaar, J., Corvera, S., 2008. Enhanced angiogenesis in obesity and in response to PPARgamma activators through adipocyte VEGF and ANGPTL4 production. Am. J. Physiol. Endocrinol. Metab. 295, E1056–E1064.
Golias, C., Tsoutsi, E., Matziridis, A., Makridis, P., Batistatou, A., Charalabopoulos, K., 2007. Review. Leukocyte and endothelial cell adhesion molecules in inflammation focusing on inflammatory heart disease. In Vivo 21, 757–769.
Koch, S., Claesson-Welsh, L., 2012. Signal transduction by vascular endothelial growth factor receptors. Cold Spring Harb. Perspect. Med 2, a006502.
Kolluru, G.K., Bir, S.C., Kevil, C.G., 2012. Endothelial dysfunction and diabetes: effects on angiogenesis, vascular remodeling, and wound healing. Int. J. Vasc. Med 2012, 918267.
Kurebayashi, S., Xu, X., Ishii, S., Shiraishi, M., Kouhara, H., Kasayama, S., 2005. A novel thiazolidinedione MCC-555 down-regulates tumor necrosis factor-alpha-induced expression of vascular cell adhesion molecule-1 in vascular endothelial cells. Atherosclerosis 182, 71–77.
Laakso, M., Kuusisto, J., 2014. Insulin resistance and hyperglycaemia in cardiovascular disease development. Nat. Rev. Endocrinol. 10, 293–302.
Li, A., Varney, M.L., Valasek, J., Godfrey, M., Dave, B.J., Singh, R.K., 2005. Autocrine role of interleukin-8 in induction of endothelial cell proliferation, survival, migration and MMP-2 production and angiogenesis. Angiogenesis 8, 63–71.
Liang, C.C., Park, A.Y., Guan, J.L., 2007. In vitro scratch assay: a convenient and inexpensive method for analysis of cell migration *in vitro*. Nat. Protoc. 2, 329–333.
Livak, K.J., Schmittgen, T.D., 2001. Analysis of relative gene expression data using real-time quantitative PCR and the 2(-Delta Delta C(T)) method. Methods 25, 402–408.
Lundberg, J.O., Gladwin, M.T., Weitzberg, E., 2015. Strategies to increase nitric oxide signalling in cardiovascular disease. Nat. Rev. Drug Discov.
Nagahama, R., Matoba, T., Nakano, K., Kim-Mitsuyama, S., Sunagawa, K., Egashira, K., 2012. Nanoparticle-mediated delivery of pioglitazone enhances therapeutic neovascularization in a murine model of hindlimb ischemia. Arterioscler. Thromb. Vasc. Biol. 32, 2427–2434.
Panigrahy, D., Singer, S., Shen, L.Q., Butterfield, C.E., Freedman, D.A., Chen, E.J., Moses, M.A., Kilroy, S., Duensing, S., Fletcher, C., Fletcher, J.A., Hlatky, L., Hahnfeldt, P., Folkman, J., Kaipainen, A., 2002. PPARgamma ligands inhibit primary tumor growth and metastasis by inhibiting angiogenesis. J. Clin. Invest. 110, 923–932.
Pardali, E., Goumans, M.J., ten, D.P., 2010. Signaling by members of the TGF-beta family in vascular morphogenesis and disease. Trends Cell Biol. 20, 556–567.
Pasceri, V., Wu, H.D., Willerson, J.T., Yeh, E.T., 2000. Modulation of vascular inflammation *in vitro* and *in vivo* by peroxisome proliferator-activated receptor-gamma activators. Circulation 101, 235–238.
Pitta, I.R., Galdino, S.L., Lima, M.C.A., 2007. Preparation of 2,4-thiazolidinedione derivatives having hypoglycemic activity. (BR 2006001826 A). Ref Type: Patent.
Polikandriotis, J.A., Mazzella, L.J., Rupnow, H.L., Hart, C.M., 2005. Peroxisome proliferator-activated receptor gamma ligands stimulate endothelial nitric oxide production through distinct peroxisome proliferator-activated receptor gamma-dependent mechanisms. Arterioscler. Thromb. Vasc. Biol. 25, 1810–1816.
Rask-Madsen, C., King, G.L., 2007. Mechanisms of disease: endothelial dysfunction in insulin resistance and diabetes. Nat. Clin. Pract. Endocrinol. Metab. 3, 46–56.
Rask-Madsen, C., King, G.L., 2013. Vascular complications of diabetes: mechanisms of injury and protective factors. Cell Metab. 17, 20–33.
Ridnour, L.A., Isenberg, J.S., Espey, M.G., Thomas, D.D., Roberts, D.D., Wink, D.A., 2005. Nitric oxide regulates angiogenesis through a functional switch involving thrombospondin-1. Proc. Natl. Acad. Sci. USA 102, 13147–13152.
Santin, J.R., Daufenback, M., Rodrigues, I., Teixeira, S.F., Muscara, S., Lins, M.N., da,R. P., I, G.S., Farsky, S.H., 2013a. Role of an indole-thiazolidine molecule PPAR pan-agonist and COX inhibitor on inflammation and microcirculatory damage in acute gastric lesions. PLoS One 8, e76894.
Santin, J.R., Uchoa, F.D., Lima, M.C., Rabello, M.M., Machado, I.D., Hernandes, M.Z., Amato, A.A., Milton, F.A., Webb, P., Neves, F.A., Galdino, S.L., Pitta, I.R., Farsky, S. H., 2013b. Chemical synthesis, docking studies and biological effects of a pan peroxisome proliferator-activated receptor agonist and cyclooxygenase inhibitor. Eur. J. Pharm. Sci. 48, 689–697.
Schaffer, S.W., Jong, C.J., Mozaffari, M., 2012. Role of oxidative stress in diabetes-mediated vascular dysfunction: unifying hypothesis of diabetes revisited. Vasc. Pharmacol. 57, 139–149.
Scoditti, E., Massaro, M., Carluccio, M.A., Distante, A., Storelli, C., De, C.R., 2010. PPARgamma agonists inhibit angiogenesis by suppressing PKCalpha- and CREB-mediated COX-2 expression in the human endothelium. Cardiovasc. Res. 86, 302–310.
Wang, N., Verna, L., Chen, N.G., Chen, J., Li, H., Forman, B.M., Stemerman, M.B., 2002. Constitutive activation of peroxisome proliferator-activated receptor-gamma suppresses pro-inflammatory adhesion molecules in human vascular endothelial cells. J. Biol. Chem. 277, 34176–34181.
Xin, X., Yang, S., Kowalski, J., Gerritsen, M.E., 1999. Peroxisome proliferator-activated receptor gamma ligands are potent inhibitors of angiogenesis *in vitro* and *in vivo*. J. Biol. Chem. 274, 9116–9121.
Zent, R., Pozzi, A., 2007. Angiogenesis in diabetic nephropathy. Semin. Nephrol. 27, 161–171.